HOME

HELP

OAK RIDGE NATIONAL LABORATORY

operated by

UNION CARBIDE CORPORATION

for the

U.S. ATOMIC ENERGY COMMISSION

UNION CARBIDE

ORNL - TM - 379

COPY NO. - 119

DATE - October 15, 1962

TEMPERATURE AND REACTIVITY COEFFICIENT AVERAGING IN THE MSRE

B. E. Prince and J. R. Engel

ABSTRACT

Use is made of the concept of "nuclear average temperature" to relate the spatial temperature profiles in fuel and graphite attained during high power operation of the MSRE to the neutron multiplication constant. Based on two-group perturbation theory, temperature weighting functions for fuel and graphite are derived, from which the nuclear average temperatures may be calculated. Similarly, importance-averaged temperature coefficients of reactivity are defined. The values of the coefficients calculated for the MSRE were $-4.4 \times 10^{-5}/°F$ for the fuel and -7.3×10^{-5} for the graphite. These values refer to a reactor fueled with salt which does not contain thorium. They were about 5% larger than the values obtained from a one-region, homogeneous reactor model, thus reflecting the variation in the fuel volume fraction throughout the reactor and the effect of the control rod thimbles on the flux profiles.

NOTICE

This document contains information of a preliminary nature and was prepared primarily for internal use at the Oak Ridge National Laboratory. It is subject to revision or correction and therefore does not represent a final report. The information is not to be abstracted, reprinted or otherwise given public dissemination without the approval of the ORNL patent branch, Legal and Information Control Department.

INTRODUCTION

Prediction of the temperature kinetic behavior and the control rod requirements in operating the MSRE at full power requires knowledge of the reactivity effect of nonuniform temperature differences in fuel and graphite throughout the core. Since detailed studies have recently been made of the core physics characteristics at isothermal (1200°F) conditions,[1] perturbation theory provides a convenient approach to this problem. Here, the perturbation is the change in fuel and graphite temperature profiles from the isothermal values. In the following section the analytical method is presented. Specific calculations for the MSRE are discussed in the final section of this report.

ANALYSIS

The mathematical problem considered in this section is that of describing the temperature reactivity feedback associated with changes in reactor power by use of average fuel and graphite temperatures rather than the complete temperature distributions. The proper averages are derived by considering spatially uniform temperatures which give the same reactivity effect as the actual profiles. The reactivity is given by the following first-order perturbation formula:[3]

$$\rho = \frac{\delta k_e}{k_e} \simeq \frac{k_e[\Phi^*, \delta M\Phi]}{[\Phi^*, F\Phi]} \tag{1}$$

Equation 1 relates a small change in the effective multiplication constant k_e to a perturbation δM in the coefficient matrix of the two-group equations. The formulation of the two-group equations which defines the terms in (1) is:

$$-D_1 \nabla^2 \phi_1 + \Sigma_{a1} \phi_1 - \frac{\nu\Sigma_{f1}}{k_e} \phi_1 - \frac{\nu\Sigma_{f2}}{k_e} \phi_2 = 0 \tag{2a}$$

$$-D_2 \nabla^2 \phi_2 + \Sigma_{a2} \phi_2 - \Sigma_{R1} \phi_1 = 0 \tag{2b}$$

or, writing (2) in matrix form:

$$M\Phi = A\Phi - \frac{F\Phi}{k_e} = 0 \qquad (3)$$

where:

$$A = \begin{pmatrix} (-D_1\nabla^2 + \Sigma_{R1} + \Sigma_{a1}) & 0 \\ -\Sigma_{R1} & -D_2\nabla^2 + \Sigma_{a2} \end{pmatrix}$$

$$F = \begin{pmatrix} \nu\Sigma_{f1} & \nu\Sigma_{f2} \\ 0 & 0 \end{pmatrix}$$

$$\Phi = \begin{pmatrix} \phi_1 \\ \phi_2 \end{pmatrix}$$

$$\delta M = \delta A - \frac{\delta F}{k_e}$$

In equation 1, Φ^* is the adjoint flux vector,

$$\Phi^* = (\phi_1^* \ \phi_2^*)$$

and the bracketed terms represent the scalar products;

$$[\Phi^*, \delta M\Phi] = \int_{Reactor} (\phi_1^* \ \phi_2^*) \begin{pmatrix} \delta M_{11} & \delta M_{12} \\ \delta M_{21} & \delta M_{22} \end{pmatrix} \begin{pmatrix} \phi_1 \\ \phi_2 \end{pmatrix} dV$$

$$= \int_{Reactor} (\phi_1^* \delta M_{11} \phi_1 + \phi_1^* \delta M_{12} \phi_2 + \phi_2^* \delta M_{21} \phi_1 + \phi_2^* \delta M_{22} \phi_2) \, dV \qquad (4)$$

A similar expression holds for $[\Phi^*, F\Phi]$ with the elements of the F matrix replacing δM.

Temperature Averaging

Starting with the critical, isothermal reactor ($k_e = 1$, $T = T_o$), consider the effects on the neutron multiplication constant of changing the fuel and graphite temperatures to $T_f(r,z)$ and $T_g(r,z)$. These effects may be treated as separate perturbations as long as $\delta k/k$ produced by each change is small. Consider first the fuel. As the temperature shifts from T_{fo} to $T_f(r,z)$, with the graphite temperature held constant, the reactivity change is:

$$\rho_f = \left.\frac{\delta k}{k}\right|_{T_{fo} \to T_f(r,z)} = - \frac{[\Phi^*, \delta M(T_{fo} \to T_f)\,\Phi]}{[\Phi^*, F\Phi]} \tag{5}$$

If the nuclear coefficients comprising the matrix M do not vary rapidly with temperature, δM can be adequately approximated by the first term in an expansion about T_{fo}, i.e.,

$$\delta M(T_{fo} \to T_f) \simeq m(T_{fo})\,(T_f - T_{fo}) \tag{6}$$

In equation (6), m is the coefficient matrix:

$$m(T_{fo}) = \left.\begin{pmatrix} \frac{\partial M_{11}}{\partial T_f} & \frac{\partial M_{12}}{\partial T_f} \\ \frac{\partial M_{21}}{\partial T_f} & \frac{\partial M_{22}}{\partial T_f} \end{pmatrix}\right|_{T_f = T_{fo}} \tag{7}$$

Thus:

$$\left.\frac{\delta k}{k}\right|_{T_{fo} \to T_f(r,z)} = - \frac{[\Phi^*, m(T_{fo})\,(T_f - T_{fo})\,\Phi]}{[\Phi^*, F\Phi]} \tag{8}$$

Now, consider a second situation in which the fuel temperature is changed from T_{fo} to T_f^* uniformly over the core. The reactivity change is:

$$\left.\frac{\delta k}{k}\right|_{T_{fo} \to T_f^*} = - \frac{[\Phi^*, \delta M(T_{fo} \to T_f^*) \Phi]}{[\Phi^*, F\Phi]}$$

$$= - \frac{[\Phi^*, m(T_{fo}) (T_f^* - T_{fo}) \Phi]}{[\Phi^*, F\Phi]} \qquad (9)$$

We may define the fuel nuclear average temperature T_f^* as the uniform temperature which gives rise to the same reactivity change as the actual temperature profile in the core, i.e.;

$$\left[\Phi^*, m(T_{fo}) (T_f^* - T_{fo}) \Phi\right] = \left[\Phi^*, m(T_{fo}) \left(T_f (r,z) - T_{fo}\right)\Phi \right] \qquad (10)$$

Since T_f^* is independent of position it may be factored from the scalar product in the left hand side of (10):

$$T_f^* = \frac{[\Phi^*, m (T_{fo}) T_f (r,z) \Phi]}{[\Phi^*, m (T_{fo}) \Phi]} \qquad (11)$$

In an analogous fashion, the nuclear average temperature for the graphite is defined by:

$$T_g^* = \frac{[\Phi^*, m (T_{go}) T_g(r,z) \Phi]}{[\Phi^*, m(T_{go}) \Phi]} \qquad (12)$$

with

$$m(T_{go}) = \begin{pmatrix} \frac{\partial M_{11}}{\partial T_g} & \frac{\partial M_{12}}{\partial T_g} \\ \frac{\partial M_{21}}{\partial T_g} & \frac{\partial M_{22}}{\partial T_g} \end{pmatrix}_{T_g = T_{go}}$$

Temperature Coefficients of Reactivity

Importance-averaged temperature coefficients may be derived which are consistent with the definitions of the nuclear average temperatures. Again consider the fuel region. Let the initial reactivity perturbation correspond to T_f assuming a profile $T_{f1}(r,z)$ about the initial value T_{fo}:

$$\rho_1 = - \frac{[\Phi^*, m(T_{fo}) \; (T_{f1}(r,z) - T_{fo}) \; \Phi]}{[\Phi^*, F\Phi]} \qquad (14)$$

If a second temperature change is now made $(T_f \rightarrow T_{f2})$,

$$\rho_2 = - \frac{[\Phi^*, m(T_{fo}) \; (T_{f2}(r,z) - T_{fo}) \; \Phi]}{[\Phi^*, F\Phi]} \qquad (15)$$

Subtracting, and using the definition (11) of the fuel nuclear average temperature:

$$\delta\rho_{21} = - \frac{\left[\Phi^*, m(T_{fo}) \left(T_{f2}(r,z) - T_{f1}(r,z)\right) \Phi\right]}{[\Phi^*, F\Phi]} \qquad (16)$$

$$= - \frac{[\Phi^*, m(T_{fo}) \; \Phi]}{[\Phi^*, F\Phi]} \left(T_{f2}^* - T_{f1}^*\right)$$

This leads to the relation defining the fuel temperature coefficient of reactivity:

$$\frac{\delta\rho}{\delta T_f^*} = - \frac{[\Phi^*, m(T_{fo}) \; \Phi]}{[\Phi^*, F\Phi]} \qquad (17a)$$

and a similar definition may be made of the graphite temperature coefficient:

$$\frac{\delta\rho}{\delta T_g^*} = - \frac{[\Phi^*, m(T_{go}) \; \Phi]}{[\Phi^*, F\Phi]} \qquad (17b)$$

It may be seen from the preceding analysis that the problem of obtaining nuclear average temperatures is reducible to the calculation of the weighting function contained in the scalar product:

$$[\Phi^*, m\Phi] = \int_{\text{Reactor}} dV \, (\phi^*, m_{11}\, \phi_1 + \phi_1^*\, m_{12}\, \phi_2 + \phi_2^*\, m_{21}\, \phi_1 + \phi_2^*\, m_{22}\, \phi_2)$$

$$= \int_{\text{Reactor}} dV \; G(r,z) \qquad (18)$$

$$G(r,z) = \Phi^*\, m\, \Phi \qquad (19)$$

In the two-group formulation, the explicit form of the m matrix is:

$$m = \begin{pmatrix} \frac{d}{dT}(-D_1\nabla^2 + \Sigma_{R1} + \Sigma_{a1} - \nu\Sigma_{f1})_{T=T_o} & -\frac{d}{dT}(\nu\Sigma_{f2})_{T=T_o} \\ -\frac{d}{dT}(\Sigma_{R1})_{T=T_o} & \frac{d}{dT}(-D_2\nabla^2 + \Sigma_{a2})_{T=T_o} \end{pmatrix} \qquad (20)$$

where the derivatives are taken with respect to the fuel or graphite temperatures in order to obtain G_f or G_g, respectively. It is convenient for numerical evaluation to rewrite the derivatives in logarithmic form; e.g.,

$$\frac{d\,\Sigma_{a2}}{dT} = \Sigma_{a2}\, \beta(\Sigma_{a2})$$

where

$$\beta(\Sigma_{a2}) = \frac{1}{\Sigma_{a2}}\,\frac{d\Sigma_{a2}}{dT} = \frac{d\,(\ell n\, \Sigma_{a2})}{dT}$$

Thus, carrying out the matrix multiplication implicit in (19):

$$G(r,z) = \beta(D_1)\left\{\phi_1^*(-D_1\nabla^2\phi_1)\right\} \qquad \text{(Fast leakage)}$$

$$+\ \beta(\Sigma_{R1})\left\{\Sigma_{R1}\,\phi_1^*\,\phi_1 - \Sigma_{R1}\,\phi_2^*\,\phi_1\right\} \qquad \text{(Slowing down)}$$

$$+ \;\beta(\Sigma_{a1}) \left\{ \Sigma_{a1}\, \phi_1^* \,\phi_1 \right\} \qquad \text{(Resonance Abs.)}$$

$$+ \;\beta(\nu\Sigma_{f1}) \left\{ -\,\nu\, \Sigma_{f1}\, \phi_1^* \,\phi_1 \right\} \qquad \text{(Resonance fission)}$$

$$+ \;\beta(\nu\Sigma_{f2}) \left\{ -\,\nu\, \Sigma_{f2}\, \phi_1^* \,\phi_2 \right\} \qquad \text{(Thermal fission)}$$

$$+ \;\beta(\Sigma_{a2}) \left\{ \Sigma_{a2}\, \phi_2^* \,\phi_2 \right\} \qquad \text{(Thermal Abs.)}$$

$$+ \;\beta(D_2) \left\{ \phi_2^* \left(-D_2 \nabla^2 \phi_2\right) \right\} \qquad \text{(Thermal Leakage)} \quad (21)$$

To evaluate the leakage terms in (21), a further simplification is obtained by using the criticality relations for the unperturbed fluxes:

$$-\,D_2 \nabla^2 \phi_2 = -\,\Sigma_{a2}\, \phi_2 + \Sigma_{R1}\, \phi_1 \qquad (22)$$

$$-\,D_1 \nabla^2 \phi_1 = -\,\Sigma_{R1}\, \phi_1 - \Sigma_{a1}\, \phi_1 + \nu\Sigma_{f1}\, \phi_1 + \nu\Sigma_{f2}\, \phi_2 \qquad (23)$$

Inserting the above relations into (21) and regrouping terms results in:

$$\begin{aligned} G(r,z) = &\Big\{ \Big(\beta\,(\Sigma_{R1}) - \beta(D_1) \Big) \Sigma_{R1} + \Big(\beta\,(\Sigma_{a1}) - \beta(D_1) \Big) \Sigma_{a1} \\ &- \Big(\beta(\nu\Sigma_{f1}) - \beta(D_1) \Big) \nu\Sigma_{f1} \Big\} \phi_1^* \,\phi_1 \\ &+ \Big\{ \Big(\beta(D_1) - \beta(\nu\Sigma_{f2}) \Big) \nu\Sigma_{f2} \Big\} \phi_1^* \,\phi_2 \\ &+ \Big\{ \Big(\beta(D_2) - \beta(\Sigma_{R1}) \Big) \Sigma_{R1} \Big\} \phi_2^* \,\phi_1 \\ &+ \Big\{ \Big(\beta(\Sigma_{a2}) - \beta(D_2) \Big) \Sigma_{a2} \Big\} \phi_2^* \,\phi_2 \end{aligned} \qquad (24)$$

Equation (24) represents the form of the weighting functions used in numerical calculations for the MSRE. The evaluation of the coefficients β for fuel and graphite is discussed in the following section.

APPLICATION TO THE MSRE: RESULTS

Utilizing a calculational model in which the reactor composition was assumed uniform, Nestor obtained values for the fuel and graphite temperature coefficients.[4] The purpose of the present study was to account for the spatial variations in temperature and composition in a more exact fashion. In this connection, two-group, 19-region calculations of fluxes and adjoint fluxes have recently been made for the MSRE,[1] using the Equipoise-3A [2,3] program. These studies refer to fuel salt which contains no thorium. The geometric model representing the reactor core configuration is indicated in Fig. 1. Average compositions of each region in this figure are given in Table 1.

The resulting flux distributions, which are the basic data required for calculation of the temperature weighting functions, are given in Figs. 2 and 3. These figures represent axial and radial traverses, along lines which intersect in the region J of Fig. 1. The intersection point occurs close to the point R = 7 in., Z = 35 in. of the grid of Fig. 1, and corresponds to the position of maximum thermal flux in the reactor.

To compute the temperature weighting functions (Eq. 24), the logarithmic derivatives

$$\beta = \frac{1}{x}\frac{dx}{dT} \qquad\qquad T = T_f, T_g$$

$$x = D, \nu\Sigma_f, \Sigma_\varepsilon, \Sigma_R$$

For each group must be numerically evaluated. Here, certain simplifying approximations may be made. It was assumed that the diffusion and slowing down parameters D and Σ_R vary with temperature only through the fuel and graphite densities and not through the microscopic cross sections. Thus, using:

$$\Sigma = \Sigma^f + \Sigma^g + \Sigma^{In}$$

ORNL-LR-Dwg 74858
Unclassified

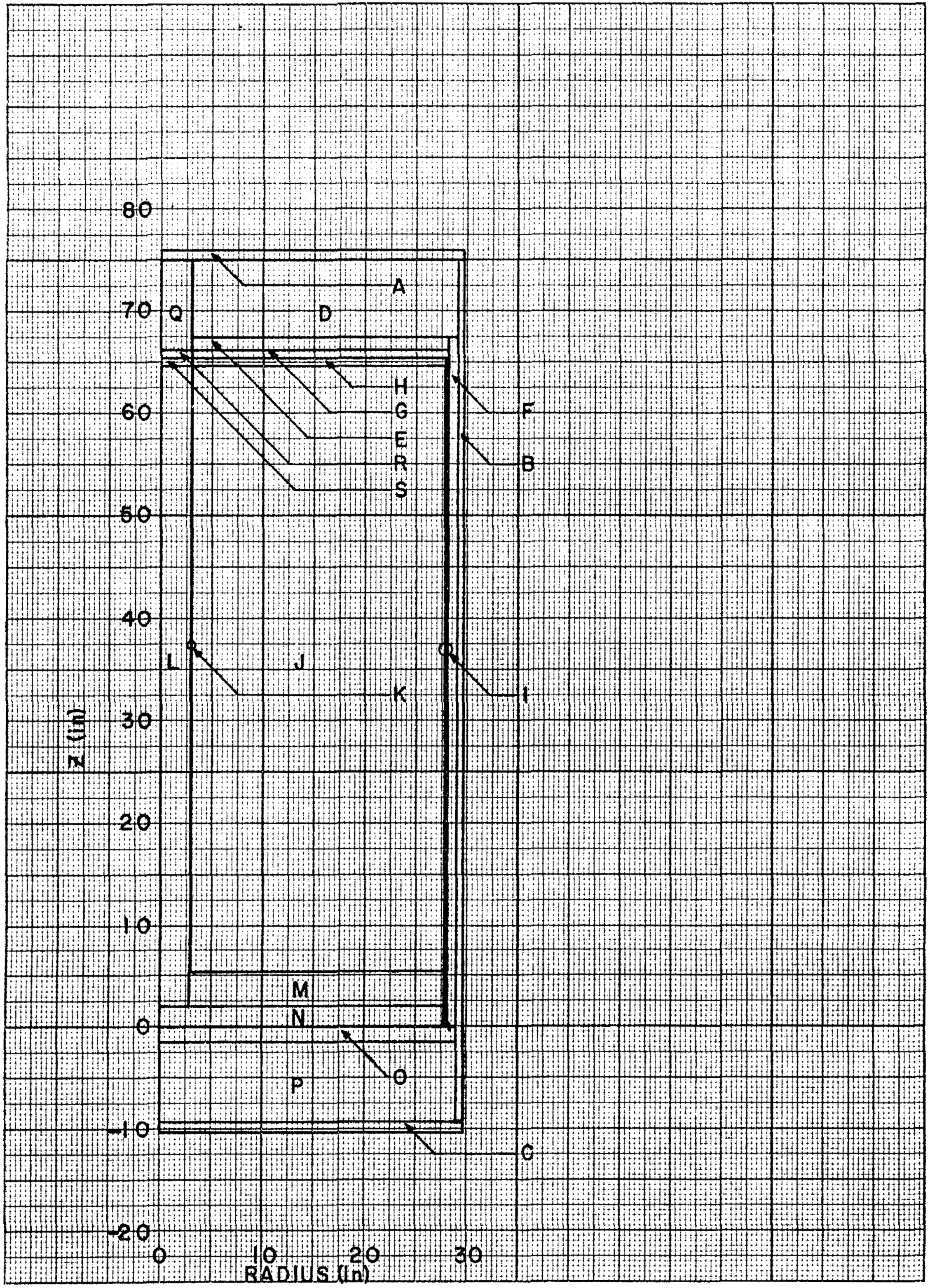

Fig. I 19-Region Core Model for Equipoise Calculation

Table 2. Nineteen-Region Core Model Used in EQUIPOISE Calculations for MSRE

Region	radius (in.)		Z (in.)		Composition (Volume percent)			Region Represented
	inner	outer	bottom	top	fuel	graphite	INOR	
A	0	29.56	74.92	76.04	0	0	100	Vessel top
B	29.00	29.56	- 9.14	74.92	0	0	100	Vessel sides
C	0	29.56	-10.26	-9.14	0	0	100	Vessel bottom
D	3.00	29.00	67.47	74.92	100	0	0	Upper head
E	3.00	28.00	66.22	67.47	93.7	3.5	2.8	
F	28.00	29.00	0	67.47	100	0	0	Downcomer
G	3.00	28.00	65.53	66.22	94.6	5.4	0	
H	3.00	27.75	64.59	65.53	63.3	36.5	0.2	
I	27.75	28.00	0	65.53	0	0	100	Core can
J	3.00	27.75	5.50	64.59	22.5	77.5	0	Core
K	2.94	3.00	5.50	74.92	0	0	100	Simulated thimbles
L	0	2.94	2.00	64.59	25.6	74.4	0	Central region
M	2.94	27.75	2.00	5.50	22.5	77.5	0	Core
N	0	27.75	0	2.00	23.7	76.3	0	Horizontal stringers
O	0	29.00	-1.41	0	66.9	15.3	17.8	
P	0	29.00	-9.14	-1.41	90.8	0	9.2	Bottom head
Q	0	2.94	66.22	74.92	100	0	0	
R	0	2.94	65.53	66.22	89.9	10.1	0	
S	0	2.94	64.59	65.53	43.8	56.2	0	

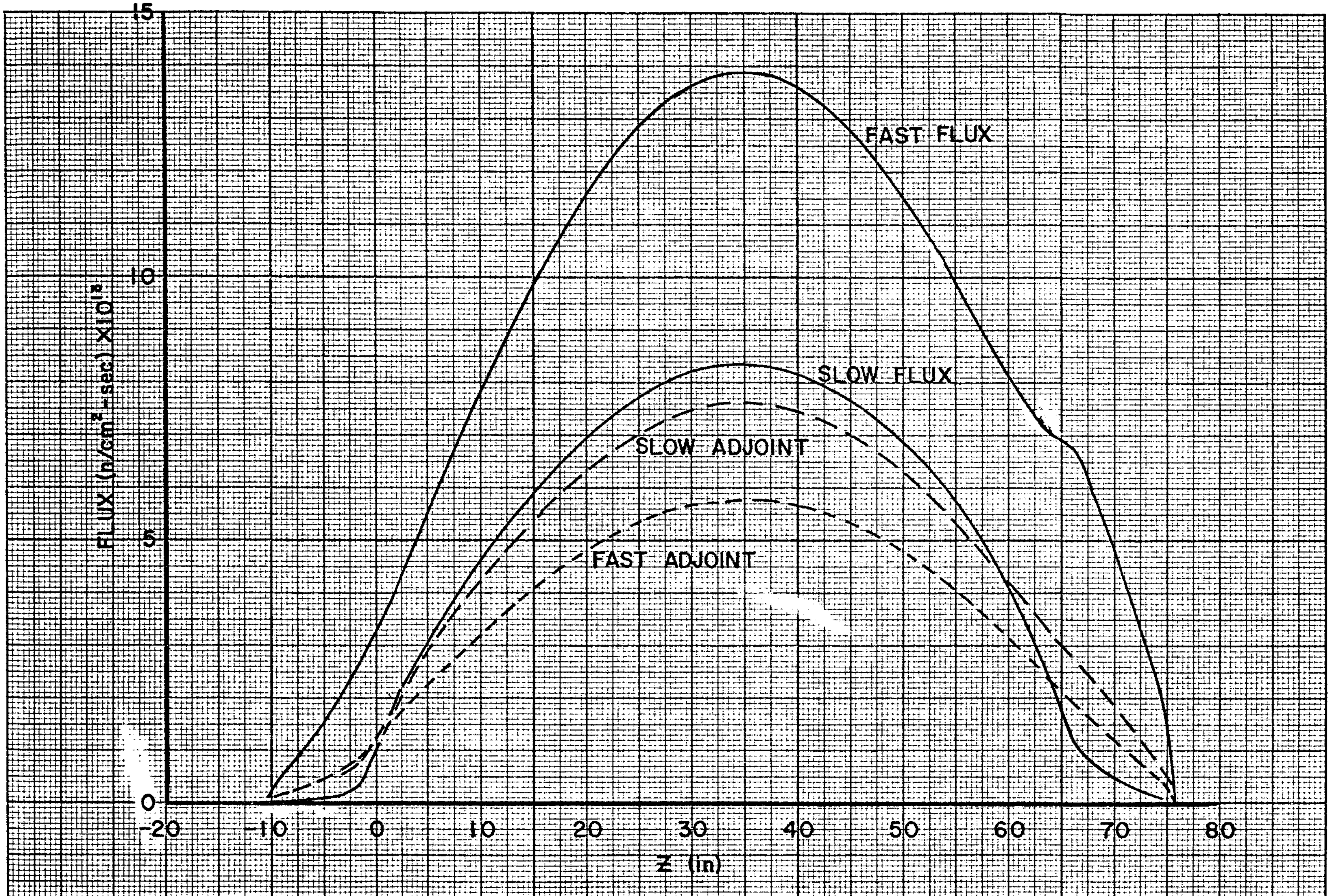

Fig. 2 Axial Distribution of Fluxes and Adjoint Fluxes At r= 7 in

ORNL-LR-Dwg 74859
Unclassified

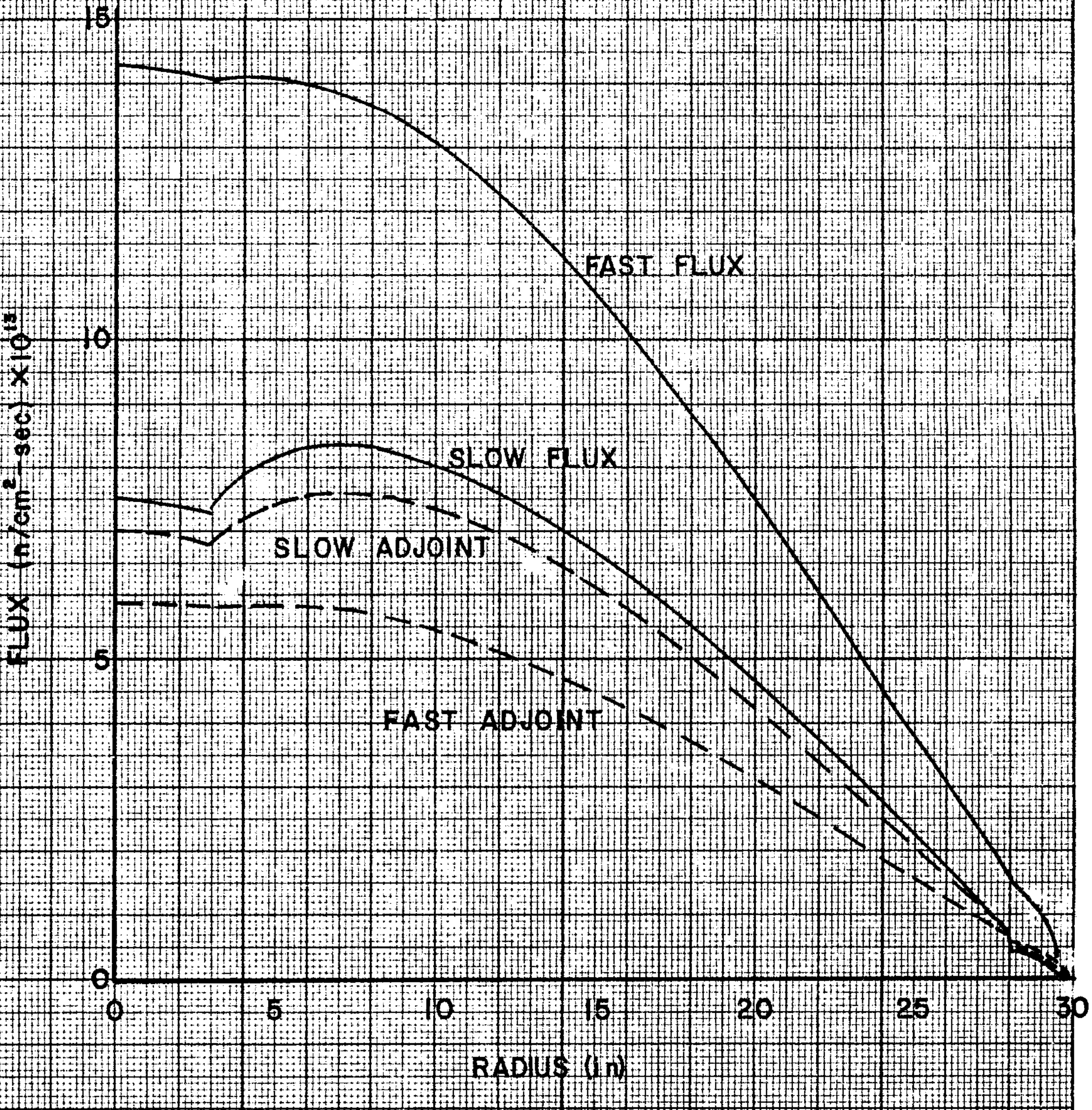

Fig. 3 Radial Distribution of Fluxes and Adjoint Fluxes At Z = 35 in

where f, g, and In refer to fuel salt, graphite, and Inor;

$$\beta(D) = \frac{1}{D}\frac{dD}{dT} = -\frac{1}{\Sigma_{tr}}\frac{d\Sigma_{tr}}{dT}$$

$$= \frac{\Sigma_{tr}^{f}}{\Sigma_{tr}}\beta\left(\Sigma_{tr}^{f}\right) + \frac{\Sigma_{tr}^{g}}{\Sigma_{tr}}\beta\left(\Sigma_{tr}^{g}\right) + \frac{\Sigma_{tr}^{In}}{\Sigma_{tr}}\beta\left(\Sigma_{tr}^{In}\right)$$

$$\simeq \frac{\Sigma_{tr}^{f}}{\Sigma_{tr}}\beta(\rho_s) + \frac{\Sigma_{tr}^{g}}{\Sigma_{tr}}\beta(\rho_g) \qquad \text{(Groups 1, 2)}$$

In the above approximation, the effect of temperature on the Inor density has also been neglected. The numerical values used for the density coefficients of fuel and graphite were:

Fuel temperature: $\beta(\rho_s) = \frac{1}{\rho_s}\frac{d\rho_s}{dT_f} = -1.26 \times 10^{-4}/°F$

$$\beta(\rho_g) = \frac{1}{\rho_g}\frac{d\rho_g}{dT_f} = 0$$

Graphite temperature: $\beta(\rho_s) = \frac{1}{\rho_s}\frac{d\rho_s}{dT_g} = 0$

$$\beta(\rho_g) = \frac{1}{\rho_g}\frac{d\rho_g}{dT_g} = -4.0 \times 10^{-6}/°F$$

The remaining coefficients were calculated as follows:

$$\beta(\nu\Sigma_{f1}) = \beta(\rho_s) + \beta(\nu\sigma_{f1})$$

$$\beta(\Sigma_{a1}) \cong \beta(\rho_s) + \beta(\sigma_{a1})$$

For the MSRE fuel, the temperature coefficients of the fuel resonance cross sections, $\beta(\nu\sigma_{f1})$ and $\beta(\sigma_{a1})$, are of the order of $10^{-5}/°F$, a factor of ten smaller than the fuel density coefficient. In addition, resonance fissions contribute only about 12% of the total fissions in the reactor. Thus $\beta(\nu\sigma_{f1})$ and $\beta(\sigma_{a1})$ were neglected in the present calculations.

For the thermal fission and absorption terms:

$$\beta(\nu\Sigma_{f2}) = \beta(\rho_s) + \beta(\nu\sigma_{f2})$$

$$\begin{aligned}\beta(\Sigma_{a2}) \simeq\ & \frac{\Sigma_{a2}{}^{25}}{\Sigma_{a2}}\left[\beta(\rho_s) + \beta(\sigma_{a2}{}^{25})\right] \\ & + \frac{\Sigma_{a2}{}^{s}}{\Sigma_{a2}}\left[\beta(\rho_s) + \beta(\sigma_{a2}{}^{s})\right] \\ & + \frac{\Sigma_{a2}{}^{g}}{\Sigma_{a2}}\left[\beta(\rho_g) + \beta(\sigma_{a2}{}^{g})\right] \\ & + \frac{\Sigma_{a2}{}^{In}}{\Sigma_{a2}}\beta(\sigma_{a2}{}^{In})\end{aligned}$$

In the above expression, the thermal cross section of the salt was separated into components; one was U^{235} and the other was the remaining salt constituents (labeled s). This was done because of the non-1/v behavior of the U^{235} cross section.

Evaluation of the temperature derivatives of the thermal cross sections gives rise to the question of the relationship between the neutron temperature T_n and the fuel and graphite temperatures, T_f and T_g. As seen from Table 1, except for the outer regions of the core, graphite comprises about 75 to 77 per cent of the core volume. Following Nestor's calculations, it was assumed that within these regions the neutron temperature was equal to the graphite temperature. These regions comprise the major part of the core volume (Table 1). For those external regions with fuel volume fractions greater than 50% (an arbitrarily chosen dividing point), the neutron temperature was assumed equal to the bulk temperature; i.e.,

$$T_n \simeq v_f T_f + v_g T_g$$

where v is the volume fraction. The cross sections were given by

$$\sigma_{a2} = \sigma_{a2}(T_o) \left(\frac{T_o}{T_n} \right)^b$$

with $b \simeq 0.54$ for U^{235} and $b = 0.50$ for the remaining salt constituents; on this basis the result for β is:

$$\beta(\sigma_{a2}) = \frac{1}{\sigma_{a2}} \frac{d\sigma_{a2}}{dT} = \left(\frac{1}{\sigma_{a2}} \frac{d\sigma_{a2}}{dT_n} \right) \frac{dT_n}{dT}$$

$$= - \frac{b}{T_n} \frac{dT_n}{dT}$$

Thus, for the fuel temperature:

$$\beta(\sigma_{a2}) = \frac{1}{\sigma_{a2}} \frac{d\sigma_{a2}}{dT_f} = 0 \qquad v_f \leq 0.50$$

$$= - \frac{v_f b}{T_o} \qquad v_f > 0.50$$

$$T_o = 1200°F$$

For the graphite temperature:

$$\beta(\sigma_{a2}) = \frac{1}{\sigma_{a2}} \frac{d\sigma_{a2}}{dT_g} = - \frac{b}{T_o} \qquad v_f \leqslant 0.50$$

$$= - \frac{v_g b}{T_o} \qquad v_f > 0.50$$

Based upon the preceding approximations, the results of calculations of the fuel and graphite temperature weighting functions are plotted in Figs. 4 through 6. Figure 4 is a radial plot, and Figs. 5 and 6 are axial plots of the fuel and graphite functions, respectively. In the latter

ORNL-LR-Dwg 74861
Unclassified

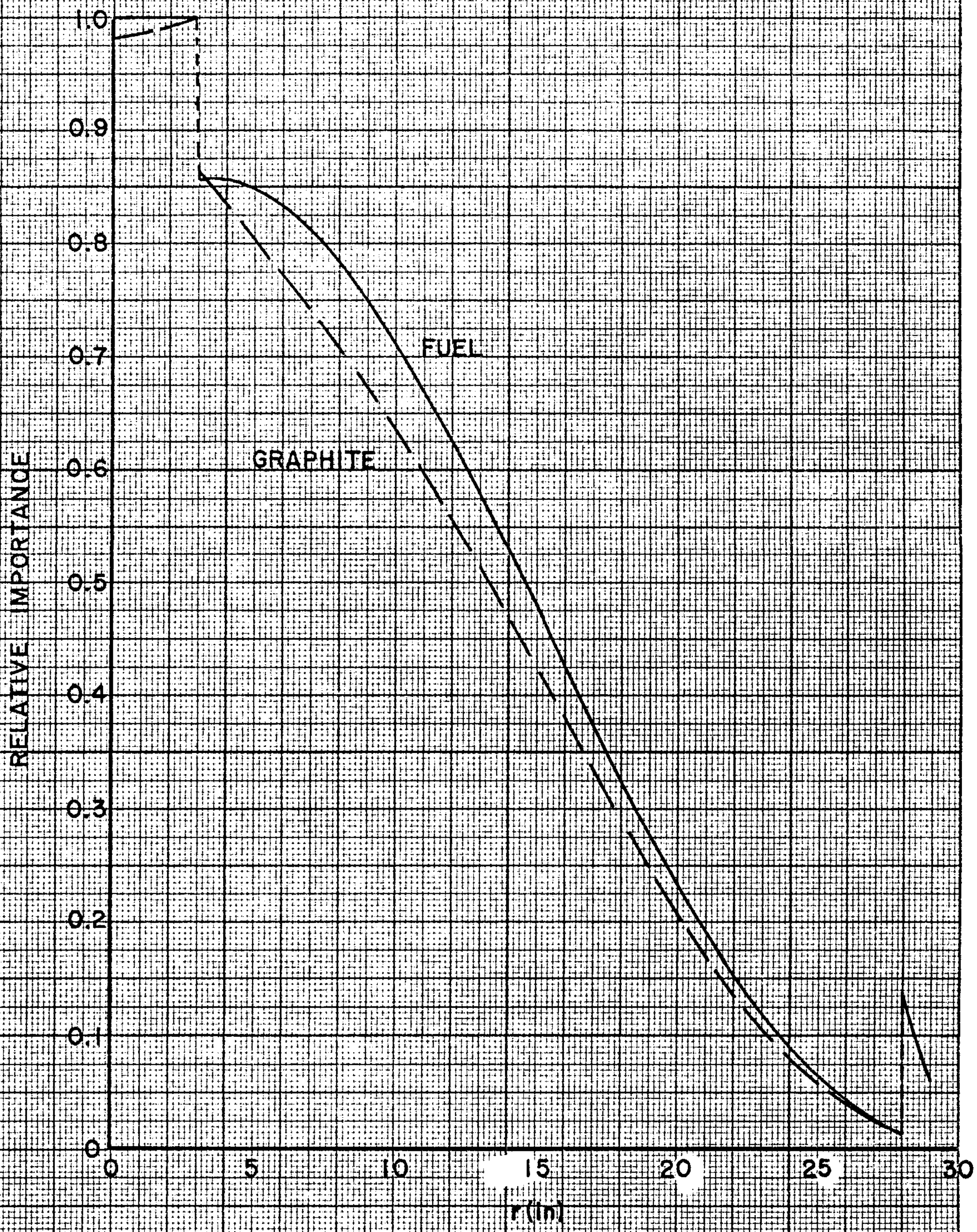

Fig. 4 Relative Radial Nuclear Importance of Fuel and Graphite Temperature Changes (At Z = 35 in)

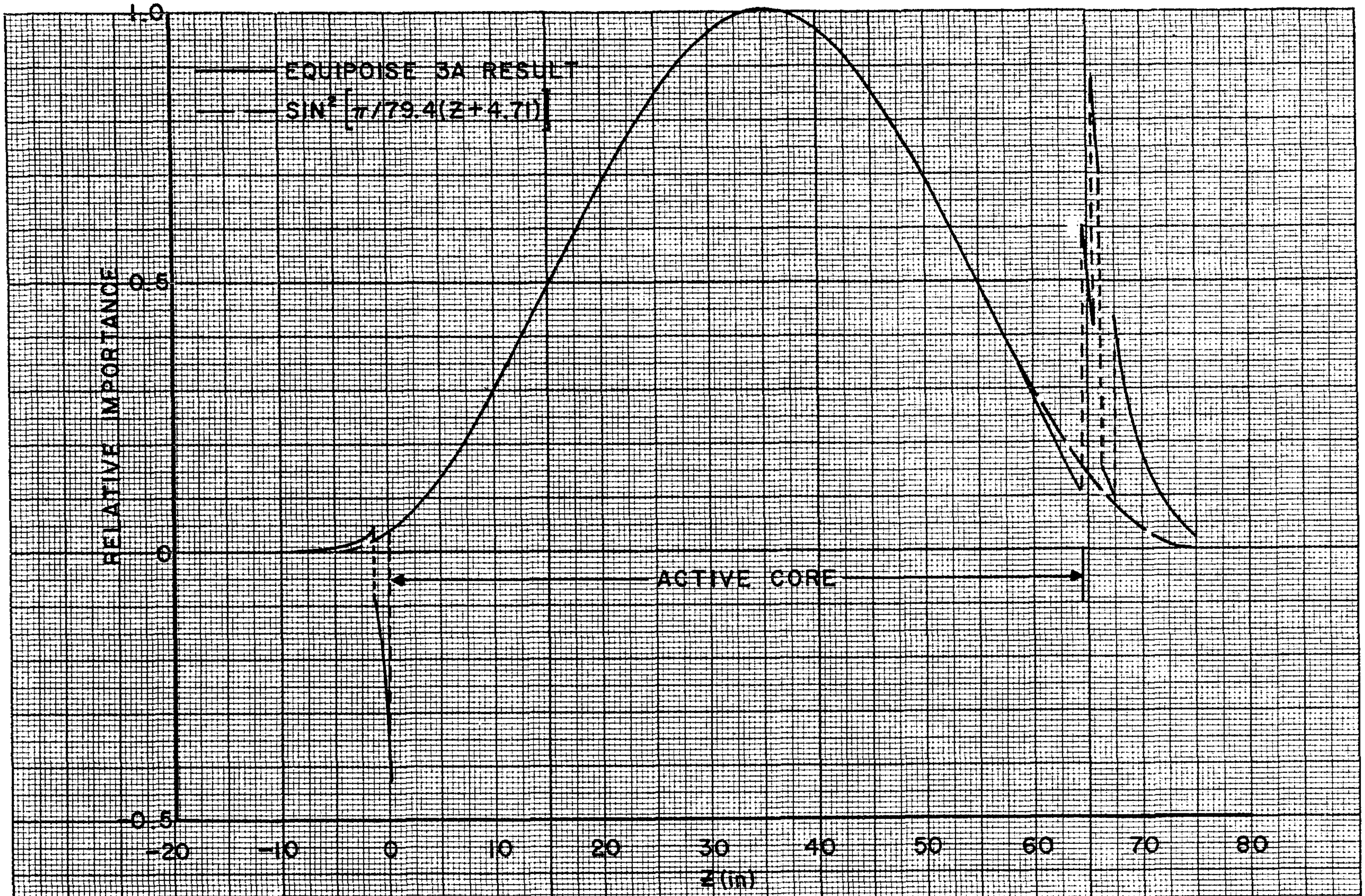

Fig. 5 Relative Axial Importance of Fuel Temperature Changes (At r = 7 in)

ORNL-LR-Dwg 74862
Unclassified

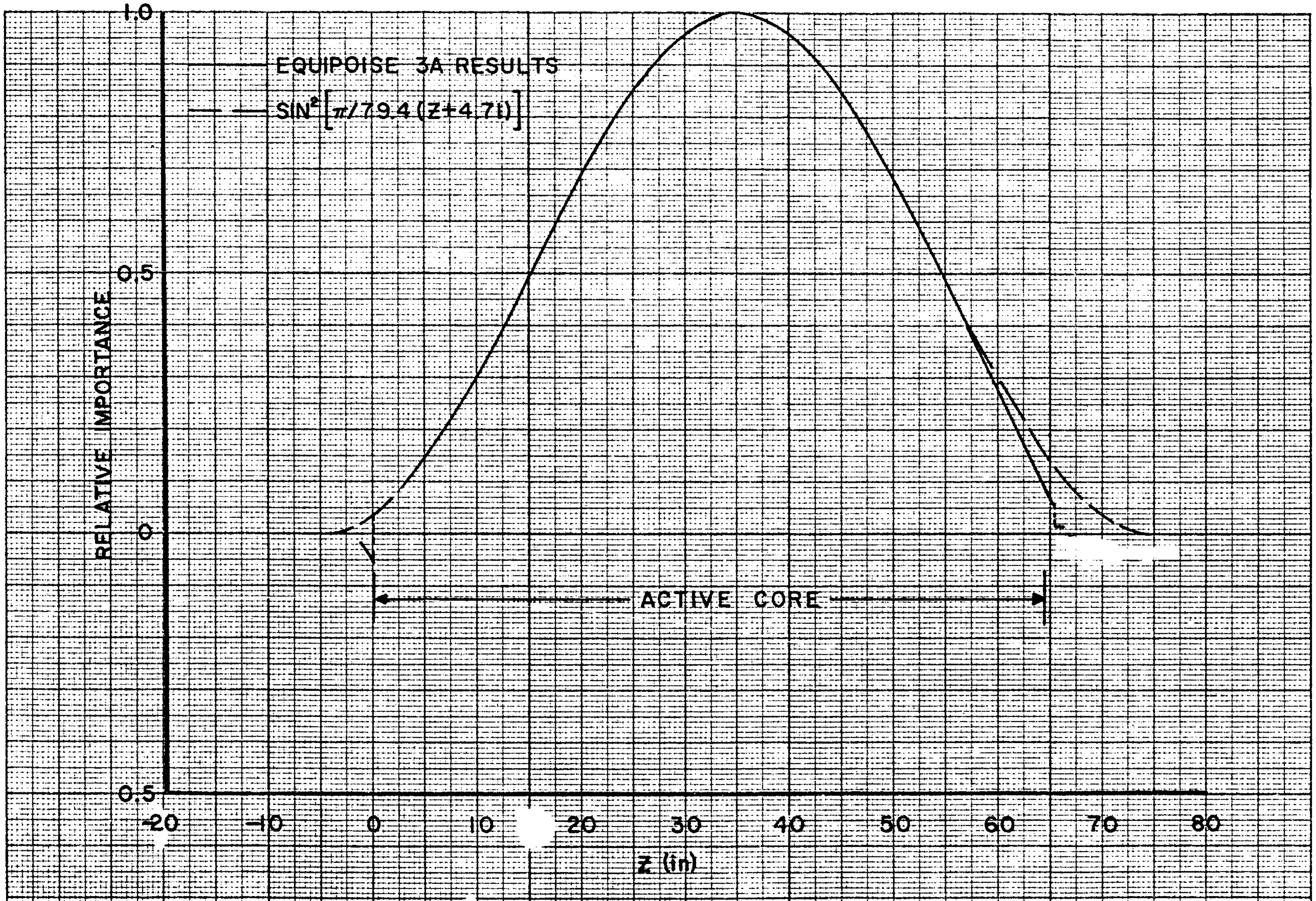

Fig. 6 Relative Axial Nuclear Importance of Graphite Temperature Changes (At r = 7 in)

ORNL-LR-Dwg 74863
Unclassified

figures, the "active core" is the vertical section over which the uniform reactor approximation, $\sin^2 \frac{\pi}{H} (z + z_o)$ may be used to represent the weight function.

Temperature coefficients of reactivity consistent with these weighting functions were calculated from Eq. 17. These values are listed in Table 2, along with the coefficients obtained from the uniform reactor model as used for the calculations reported in reference (4). In the latter case, a uniform fuel volume fraction of 0.225 was used; i.e., that of the largest region in the reactor. Also, the effective radius and height of the reactor were chosen as closely as possible to correspond to the points where the Equipoise thermal fluxes extrapolate to zero from the active core.

Table 2. MSRE Temperature Coefficients of Reactivity

	Fuel 10^{-5}/°F	Graphite 10^{-5}/°F
Perturbation theory	-4.45	-7.27
Homogeneous reactor model	-4.13	-6.92

APPLICATION TO THE MSRE - DISCUSSION OF RESULTS

The relative importance of temperature changes on the reactivity varies from region to region in the reactor due to two effects. One is the change in the nuclear importance, as measured by the adjoint fluxes. The other is the variation in the local infinite multiplication constant as the fuel-graphite-Inor 8 composition varies. The latter effect leads to the discontinuities in the temperature weighting function. For example, region 0 of Fig. 1 contains a relatively large volume fraction of Inor 8 (see Table 1). This results in net subcriticality of this region in the absence of the net inleakage of neutrons from the surrounding regions. Thus the reactivity effect of a temperature increment in this region has the opposite sign from that of the surroundings.

It should be understood that the validity of the perturbation calculations in representing the local temperature-reactivity effects depends upon how accurately the original flux distributions and average region compositions represent the nuclear behavior of the reactor. Also, it was necessary to assume a specific relation between the local neutron temperature and the local fuel and graphite temperatures. More exact calculations would account for a continuous change in thermal spectrum as the average fuel volume fraction changes. This would have the effect of "rounding off" the discontinuities in the temperature weighting functions. These effects, however should be relatively minor and the results presented herein should be a reasonably good approximation.

Nuclear average temperatures have been calculated from computed MSRE temperature distributions, using the weighting functions given in this report and are reported elsewhere.[5]

NOMENCLATURE

k_e	Static multiplication constant
A	Coefficient matrix of absorption plus leakage terms in diffusion equations
F	Coefficient matrix of neutron production terms in diffusion equations
M	Matrix of nuclear coefficients in diffusion equations for unperturbed reactor
m	Temperature derivative of M matrix
$G(r,z)$	Temperature weighting functions of position: Subscripts f = fuel salt, g = graphite
D_j	Diffusion coefficient, group j = 1,2
T	Temperature: Subscripts f = fuel salt, g = graphite, o = initial, n = effective thermal neutron temperature
T^*	Nuclear average temperature
dV	Reactor volume element
v	Volume fraction
ϕ_j	Neutron flux, groups j = 1, 2
Φ	Neutron flux vector
ϕ_j^*	Adjoint flux, groups j = 1, 2
Φ^*	Adjoint flux vector
ρ	Reactivity
ρ_s	Density of fuel salt
ρ_g	Density of reactor graphite
$\sum_j$	Macroscopic cross section, groups j = 1, 2; Subscripts a = absorption, f = fission, R = removal
$\beta(x)$	Temperature derivative of ℓn x
ν	Number of neutrons per fission

REFERENCES

1. MSRP Prog. Rep. August 31, 1962, (ORNL report to be issued).

2. T. B. Fowler and M. L. Tobias, Equipoise-3: A Two-Dimensional, Two-Group, Neutron Diffusion Code for the IBM-7090 Computer, ORNL-3199, Feb. 7, 1962.

3. C. W. Nestor, Jr., Equipoise 3A, ORNL-3199 Addendum, June 6, 1962.

4. MSRP Prog. Rep. August 31, 1961, ORNL-3215, p. 83.

5. J. R. Engel and P. N. Haubenreich, Temperatures in the MSRE Core During Steady State Power Operation, ORNL-TM-378 (in preparation).

gcb

Internal Distribution

1-2. MSRP Director's Office.
Rm. 219, Bldg. 9204-1
3. G. M. Adamson
4. L. G. Alexander
5. S. E. Beall
6. M. Bender
7. C. E. Bettis
8. E. S. Bettis
9. D. S. Billington
10. F. F. Blankenship
11. E. G. Bohlmann
12. S. E. Bolt
13. C. J. Borkowski
14. C. A. Brandon
15. F. R. Bruce
16. O. W. Burke
17. S. Cantor
18. T. E. Cole
19. J. A. Conlin
20. W. H. Cook
21. L. T. Corbin
22. G. A. Cristy
23. J. L. Crowley
24. F. L. Culler
25. J. H. DeVan
26. R. G. Donnelly
27. D. A. Douglas
28. N. E. Dunwoody
29. J. R. Engel
30. E. P. Epler
31. W. K. Ergen
32. D. E. Ferguson
33. A. P. Fraas
34. J. H. Frye
35. C. H. Gabbard
36. R. B. Gallaher
37. B. L. Greenstreet
38. W. R. Grimes
39. A. G. Grindell
40. R. H. Guymon
41. P. H. Harley
42. C. S. Harrill
43. P. N. Haubenreich
44. E. C. Hise
45. H. W. Hoffman
46. P. P. Holz
47. L. N. Howell
48. J. P. Jarvis
49. W. H. Jordan
50. P. R. Kasten
51. R. J. Kedl
52. M. T. Kelley
53. M. J. Kelly
54. S. S. Kirslis
55. J. W. Krewson
56. J. A. Lane
57. W. J. Leonard
58. R. B. Lindauer
59. M. I. Lundin
60. R. N. Lyon
61. H. G. MacPherson
62. F. C. Mainenschein
63. E. R. Mann
64. W. B. McDonald
65. H. F. McDuffie
66. C. K. McGlothlan
67. A. J. Miller
68. E. C. Miller
69. R. L. Moore
70. J. C. Moyers
71. T. E. Northup
72. W. R. Osborn
73. P. Patriarca
74. H. R. Payne
75. A. M. Perry
76. W. B. Pike
77. B. E. Prince
78. J. L. Redford
79. M. Richardson
80. R. C. Robertson
81. T. K. Roche
82. H. W. Savage
83. A. W. Savolainen
84. J. E. Savolainen
85. D. Scott
86. C. H. Secoy
87. J. H. Shaffer
88. M. J. Skinner
89. G. M. Slaughter
90. A. N. Smith
91. P. G. Smith
92. I. Spiewak
93. J. A. Swartout
94. A. Taboada
95. J. R. Tallackson
96. R. E. Thoma
97. D. B. Trauger
98. W. C. Ulrich

Internal Distribution - cont'd

99. B. S. Weaver
100. C. F. Weaver
101. B. H. Webster
102. A. M. Weinberg
103. J. C. White
104. L. V. Wilson
105. C. H. Wodtke
106-107. Reactor Division Library
108-109. Central Research Library
110. Document Reference Section
111-113. Laboratory Records
114. ORNL-RC

External

115-116. D. F. Cope, Reactor Division, AEC, ORO
117. H. M. Roth, Division of Research and Development, AEC, ORO
118. F. P. Self, Reactor Division, AEC, ORO
119-133. Division of Technical Information Extension, AEC, ORO
134. J. Wett, AEC, Washington
135. W. L. Smalley, AEC-ORO